Wind and Structures, *Vol. 24, No. 1 (2017) 79-93*
DOI: https:// doi.org/10.12989/was.2017.24.1.079

The loss coefficient for fluctuating flow through a dominant opening in a building

Haiwei Xu[a], Shice Yu[*] and Wenjuan Lou[b]

College of Civil Engineering and Architecture, Zhejiang University, Hangzhou 310058, China

(Received March 10, 2015, Revised November 23, 2016, Accepted November 29, 2016)

Abstract. Wind-induced fluctuating internal pressures in a building with a dominant opening can be described by a second-order non-linear differential equation. However, the accuracy and efficiency of the governing equation in predicting internal pressure fluctuations depend upon two ill-defined parameters: inertial coefficient C_I and loss coefficient C_L, since C_I determines the un-damped oscillation frequency of an air slug at the opening, while C_L controls the decay ratio of the fluctuating internal pressure. This study particularly focused on the value of loss coefficient and its influence factors including: opening configuration and location, internal volumes, as well as wind speed and approaching flow turbulence. A simplified formula was presented to predict loss coefficient, therefore an approximate relationship between the standard deviation of internal and external pressures can be estimated using Vickery's approach. The study shows that the loss coefficient governs the peak response of the internal pressure spectrum which, in turn, will directly influence the standard deviation of the fluctuating internal pressure. The approaching flow characteristic and opening location have a remarkable effect on the parameter C_L.

Keywords: wind tunnel test; dominant opening; internal pressure; loss coefficient; Helmholtz resonance

1. Introduction

Strong wind actions on a building in the presence of a dominant opening may produce a large internal pressure which is as much important as the external pressure with regard to its effect on building safety. Ignoring the contribution of this internal pressure in building design can lead to an underestimation of net wind pressure on the building envelope and cause failures during severe wind storms. Therefore, the necessity of an understanding, and appropriate evaluation, of wind-induced internal pressure are highlighted. Internal pressures are not only dependent on external pressures driving the airflow in and out of the opening but are also related to physical building features such as: opening sizes and effective internal volumes both of which will influence frequency response characteristics of a building. Numerous researchers have studied the characteristics of internal pressure response and have presented different equations to describe internal pressure fluctuations. Holmes (1979) thought wind-induced internal pressure response behaved like a Helmholtz acoustic resonator and innovatively used a second order nonlinear

∗Corresponding author, Researcher, E-mail: yusc@zju.edu.cn
[a] Dr., Email: haiweix@zju.edu.cn
[b] Professor, Email: louwj@zju.edu.cn

Copyright © 2017 Techno-Press, Ltd.
http://www.techno-press.org/?journal=was&subpage=8 ISSN: 1226-6116 (Print), 1598-6225 (Online)

differential equation to characterize it. Using the unsteady form of the Bernoulli equation, Vickery (1986) derived a similar governing equation for internal pressure and incorporated a loss coefficient C_L for the first time to represent energy loss of an oscillating air slug at the opening.

The parameter was also adopted by Sharma *et al*. (1997a) in his new differential equation which introduced an additional linear damping term to explain frictional shear losses at the opening and was more applicable to long openings. Regardless of choice of equation, satisfactory predictions of internal pressure can be obtained with appropriate C_I and C_L values. However, the two parameters vary significantly from one equation to another. Compared to the inertial coefficient which seems to have similar reference values (Xu, Yu *et al*. 2014), the loss coefficient has more variable values. According to potential flow theory, 2.78 was once generally used as the standard value of C_L by Liu and Saathoff (1981) and Vickery (1986). To match the resonant peak in the measured internal pressure spectrum, Holmes (1979) suggested 45 as a suitable loss coefficient under unsteady high fluctuation conditions: this was also supported by Ginger, Mehta *et al*. (1997) and Ginger, Holmes *et al*. (2008) through full-scale TTU field measurement. Based on CFD numerical simulation and parallel model tests of transient internal pressures, Sharma and Richards (1997c) classified the parameter C_L by opening location and the ratio of physical opening length l_0 to effective radius $r = \sqrt{A_0/\pi}$. For long openings ($l_0/r > 1.0$) and thin openings ($l_0/r < 1.0$), C_L is equal to 1.5 and 1.2, respectively. Oh, Kopp *et al*. (2007) derived a parameter value ($C_L = 2.5$) similar to that of Vickery from a series of wind tunnel tests on models with openings. Yu *et al*. (2006) studied a frequency domain method of estimating fluctuating internal pressure inside a building with a single windward wall opening and showed that $C_L = 7.5$ could also produce favourable simulation coefficients to match measured data. Ginger and Holmes (2010) found that C_L varied from 6.25 to 100 with variation of dominant opening sizes and volumes.

To understand the behaviour of internal pressure response and make better use of the governing equation, the parameter C_L must first be determined. In this study, possible influence factors including: the opening configuration and position, the building internal volume, wind speed, and turbulence intensity in the incoming flow were investigated by wind tunnel tests to establish an empirical formula to give a reasonable approximation of the loss coefficient. With accurate loss coefficients, validity of a simplified equation proposed by Vickery and Bloxham (1992) to estimate the standard deviation of the internal pressure were verified using experimental data.

2. Governing equation

Based on unsteady orifice flow theory, Vickery (1986) described the relationship between internal and external pressure with a second-order non-linear differential equation

$$\frac{\rho_a l_e V_0}{\gamma A_0 P_a}\ddot{C}_{pi} + \frac{C_L \rho_a V_0^2 q}{2\gamma^2 A_0^2 P_a^2}\dot{C}_{pi}\left|\dot{C}_{pi}\right| + C_{pi} = C_{pe} \tag{1}$$

The corresponding Helmholtz resonant frequency f_{H} is given by

$$f_{\mathrm{H}} = \frac{1}{2\pi}\sqrt{\frac{\gamma A_0 P_a}{\rho_a V_0 l_{\mathrm{e}}}} \tag{2}$$

$C_{pi} = P_{\mathrm{i}}/q$ and $C_{pe} = P_{\mathrm{e}}/q$ are internal and external pressure coefficients, respectively. The

reference dynamic pressure $q = 0.5\rho_a U_h^2$ where U_h is the mean wind velocity at the reference height. ρ_a and P_a are the mass density and pressure of the air ,respectively. γ is the specific heat ratio, A_0 is the opening size, V_0 is the internal volume of the model, $l_e = l_0 + C_I\sqrt{A_0}$ is the effective length of the air slug at the orifice. The Eq. (1) is quite similar to the one proposed by Holmes except for the parameter C_L in the damping term which was replaced by $1/k^2$ (k is the discharge coefficient), therefore the corresponding results for the parameter k can be obtained from the relationship $C_L = 1/k^2$.

Using dimensional analysis suggested by Holmes (1979), Eq. (1) can be rewritten as a function of several non-dimensional parameters

$$\frac{C_I}{S^*\Phi_5^2}\frac{d^2C_{pi}}{dt^{*2}} + \frac{C_L}{4S^{*2}\Phi_5^2}\frac{dC_{pi}}{dt^*}\left|\frac{dC_{pi}}{dt^*}\right| + C_{pi} = C_{pe} \tag{3}$$

where $\Phi_1 = A_0^{3/2}/V_0$, $\Phi_2 = \alpha_s / U_h$, $\Phi_3 = \rho_a U_h\sqrt{A_0} / \mu$, $\Phi_4 = \sigma_U / U$, $\Phi_5 = \lambda/\sqrt{A_0}$, $S^* = \Phi_1\Phi_2^2$, and $t^* = tU_h/\lambda$, α_s is the speed of sound, λ is the integral length scale of the turbulence, t^* is the non-dimensional time, μ is the dynamic viscosity of air, and U and σ_u are the mean and root-mean-square wind speeds at given elevation, respectively. After a series of simplifications, Eq. (3) shows that the internal pressure coefficients are ultimately related to parameters C_I, C_L, Φ_5, and S^*. However, without knowing the exact values of the parameter C_I and C_L, it's difficult to determine internal pressure for a specific situation in a predictive manner.

3. Sensitivity of fluctuating internal pressure to loss coefficient

To assess the sensitivity of internal pressure fluctuation to the loss coefficient, buildings with various central windward dominant openings and internal volumes were used for numerical study. The details of building features are listed in Table 1.

Simulated wind characteristics: mean wind speed profile $U = 31.3\times(Z/10)^{0.12}$, turbulence intensity profile $I = 0.08\times(Z/300)^{-0.17}$, the theoretical Kaimal spectrum $S_u(f) = 587.8\times(\frac{z}{\overline{U}_z} / (1+50\frac{fz}{\overline{U}_z})^{5/3})$ is adopted for simulating the approach velocity fluctuations, Z and $\overline{U}_z$ are the simulation height (Z=2 m) and the corresponding mean wind speed, respectively. Simulated wind speed time series are shown in Fig. 1. In order to check the validity of simulation results, spectrum of simulated wind speed is compared with its theoretical counterpart in Fig. 2 which shows a good agreement between two spectra.

Other salient parameters for simulation were: ρ_a = 1.22 kg/m^3; P_a = 101300 Pa; γ = 1.4; reference pressure q = 600 Pa; C_I = 0.8; and $l_e = C_I\sqrt{A_0}$. For each model in Table 1, C_L = 1, 5, 10, 50, and 100 were considered respectively to calculate internal pressure coefficients from Eq. (1) using a fourth order Runge-Kutta scheme. Internal pressure spectra for Model 1 were plotted in Fig. 3 which indicated that the loss coefficient dominated the sharpness of the spectral peak at the Helmholtz frequency and resonant effects were considerably reduced as C_L increased, implying that a damping effect related to energy losses increased from low to high C_L values. Therefore,

using a small loss coefficient, such as C_L=2.87 stemmed from free streamline theory, may largely overestimate the resonance response of internal pressure under highly unsteady flow.

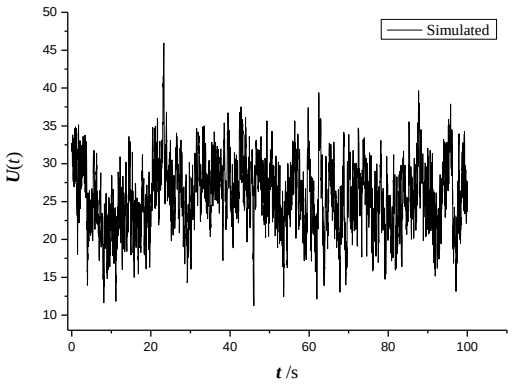

Fig. 1 Wind speed time series

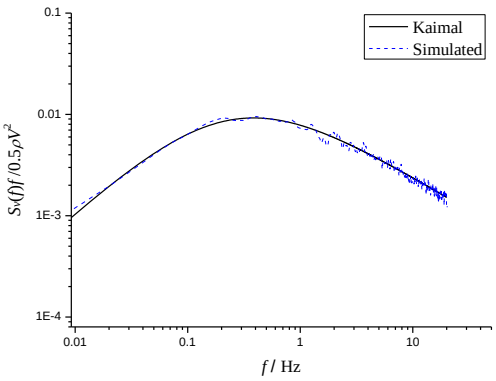

Fig. 2 Simulated and theoretical wind speed spectra

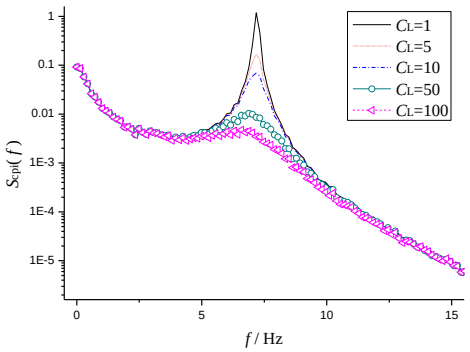

Fig. 3 Internal pressure spectrum *versus* C_L

Table 1 Building details

Model	A_0/ m^2	V_0/ m^3
1	1	200
2	2	200
3	4	200
4	8	200
5	8	400
6	8	800
7	8	1600

The ratios of standard deviation of internal to external pressure along with various C_L values for Models 1 to 7 are given in Figs. 4 and 5. The fluctuation of internal pressure decreased rapidly even if there was some increase in loss coefficient and became less sensitive to larger C_L values (such as C_L = 50 or 100). It could also be concluded from Fig. 3 where the reduction in the spectral peak of internal pressure became less obvious as the loss coefficient increased, indicating the energy loss rate of the oscillating air slug at the opening was in decline for increasing damping ratio. Comparison of Figs. 4 and 5 shows that smaller opening size or larger internal volume can decelerate the decay ratio of $\sigma_{cpi}/\sigma_{cpe}$. In another words, the effect of C_L on σ_{cpi} for a building with a small opening, but a large internal volume, will be significantly diminished. This is because a building with such characteristics will result in a larger oscillation damping at the opening.

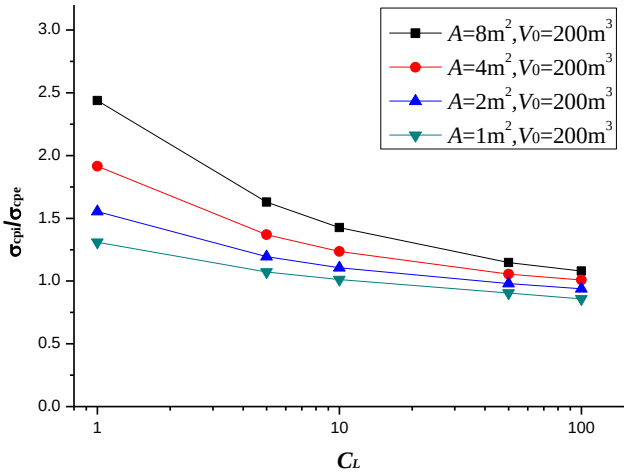

Fig. 4 $\sigma_{cpi}/\sigma_{cpe}$ *versus* C_L for different opening sizes

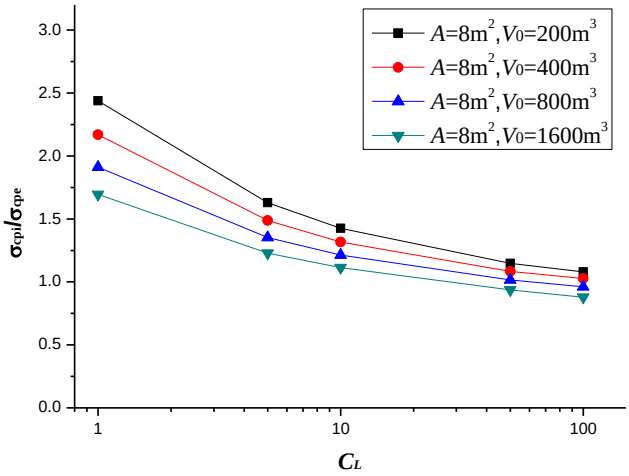

Fig. 5 $\sigma_{cpi}/\sigma_{cpe}$ *versus* C_L for different internal volumes

4. Wind tunnel investigations

To understand the effects of opening size and location, building internal volume and external wind characteristics on the loss coefficient, a 1 cm thick Perspex model with the dimensions of 36.4 cm× 54.8 cm × 16 cm (length × width × height) was tested in the boundary layer wind tunnel at Zhejiang University. Picture of the wind tunnel test model was shown in Fig. 6. Four central opening configurations including: A1 (20 cm (W) × 10 cm (H)), A2 (10 cm (W) × 10 cm (H)), A3 (5 cm (W) × 10 cm (H)), A4 (5 cm (W) × 5 cm (H)) combined with internal volumes V_0, $1.5V_0$, $2V_0$, $3V_0$, $4V_0$, and $4.5V_0$ (V_0 is the internal volume of the experiment model) were investigated at incident wind azimuths of 0° to 90° (see Fig. 7) during experiments. The internal volume of the test model can be increased by attaching a 55 cm (L) × 36 cm (W) × 55 cm (H) adjustable chamber under the turntable as shown in Fig. 7.

Fig. 6 Wind tunnel test model

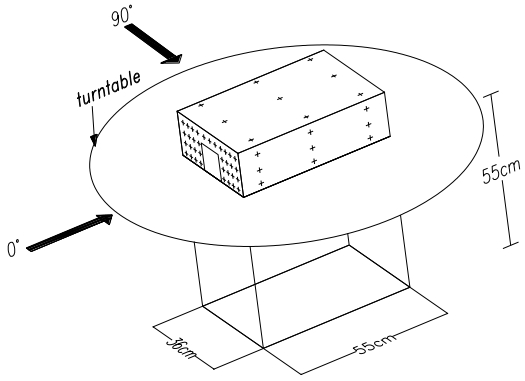

Fig. 7 Sketch of the Perspex® model

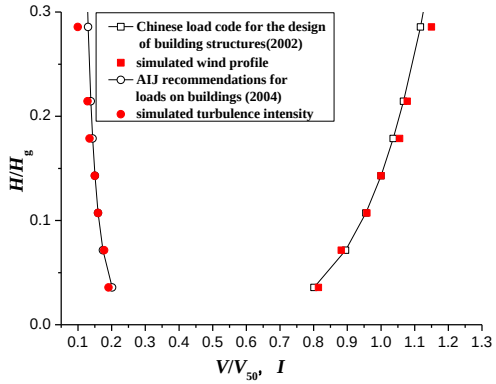

Fig. 8 Simulated mean wind velocity and turbulence intensity profile

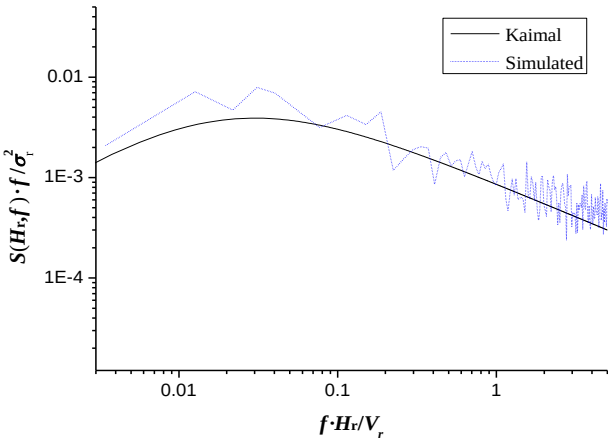

Fig. 9 Wind velocity spectrum at roof height

An atmospheric boundary layer representing Terrain Category B in the Chinese Load Code for the Design of Building Structures (2002) was simulated at a length scale of 1:250. Non-dimensional mean velocity and turbulence intensity profiles are plotted in Fig. 8 where H_g is the gradient height of the boundary layer and V_{50} represents the wind velocity at the height of 125 m in prototype. It exhibited a reasonable agreement between simulated wind filed and the code provisions (2002, 2004). Fig. 9 compares the non-dimensional longitudinal velocity spectrum measured at roof height (H_r) with the target Kaimal spectrum, where V_r and σ_r represent mean and standard deviation of wind speed at roof height, respectively. As can be seen from Fig. 9, experimental spectrum matches well with its theoretical counterpart. The measured mean wind velocity and turbulence intensity at roof height of the model were about 12.8 m/s and 16%, respectively. The integral length scale of turbulence λ in the wind tunnel was approximate 0.6 m.

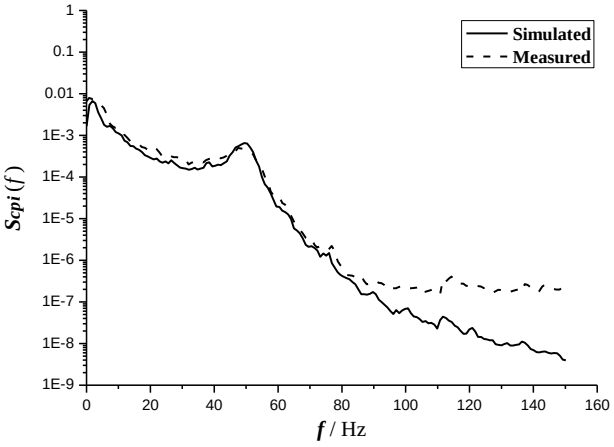

Fig. 10 Theoretical and experimental spectra of internal pressure for opening A1 and volume $4.5V_0$

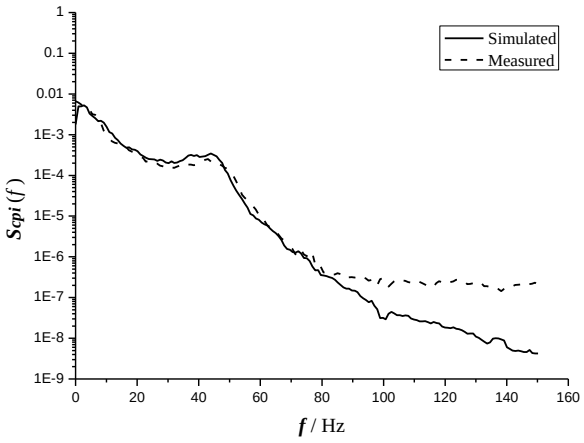

Fig. 11 Theoretical and experimental spectra of internal pressure for opening A4 and volume $2V_0$

Pressure taps were uniformly distributed on the building surfaces and ZOC33 digital modules from Scanivalve Inc were used to acquire pressure data from each tap at a sampling frequency of 625 Hz for 32 s. The original signal data were low-pass filtered at 300 Hz. External pressures were obtained by area-averaging taps on the 36 cm long windward wall when the model was sealed. Then, C_L can be identified by fitting the best internal pressure spectrum to match that measured. Figs. 10 and 11 plotted the spectra of measured internal pressure for opening A1 and A4 along with the corresponding theoretical ones estimated using identified C_L. The fitting results are satisfactory, although obvious differences are observed at high frequencies (e.g., f >90 Hz) due to the interference of background noise, verifying the reliability of the loss coefficients obtained. The outcomes for the wind direction of 0° were used in the following discussion.

Variations of the parameter C_L with S^* were illustrated in Fig. 12 which showed C_L increased with S^* and basically lay between 8 and 234 for given S^*, which was a little bit higher than that ($6.25 \leq C_L \leq 100$) given by Ginger and Holmes *et al* (2010). The differences may be attributed to different opening sizes and approaching flow characteristics adopted in the experiments. For example, the values of parameter S^* investigated in this paper are much larger than previous study and thereby result in larger values of C_L. The influence of external wind characteristics on loss coefficient will be discussed in following sections.

From the relationship of k and C_L, it could be inferred that the discharge coefficient k experienced a decreasing trend for increasing S^* and varied between 0.07 and 0.35 close to the findings ($0.1 \leq k \leq 0.4$) presented by Ginger, Holmes *et al*. (2010). However, they were much smaller than the recommended value (k=0.6) for the ideal separated flow through a circular sharp edged orifice, because the potential flow condition was not applicable to high turbulent three-dimensional reverse flow under which more energy losses would be caused when flow passed through the opening. Therefore, for unsteady high turbulence flow induced internal pressures, the value of $C_L=1/0.6^2=2.78$ used by previous studies may be inadequate.

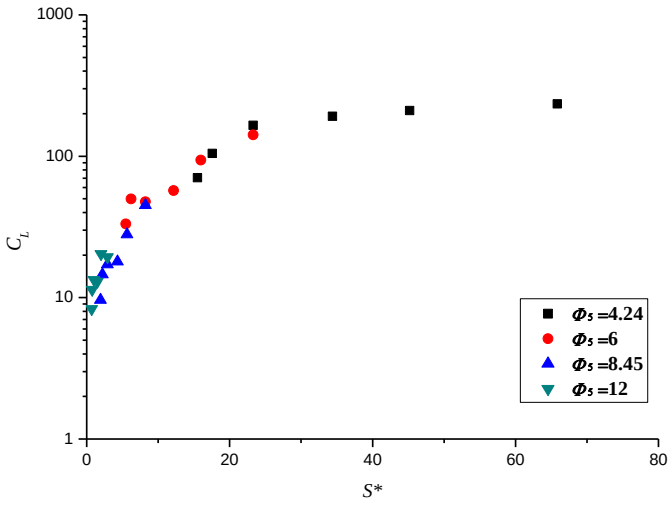

Fig. 12 C_L *versus* S^*

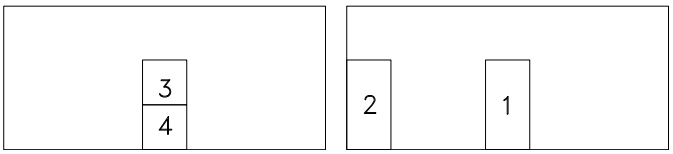

Fig. 13 Sketch of opening location(s) in the windward wall

In order to discuss the effects on loss coefficient of changes in wind velocity, turbulence intensity, and opening location, models with internal volume V_0 were selected for further study. Turbulence intensity and mean wind velocity at the model roof height were increased to 20% and reduced to 7.5 m/s, respectively. Besides, four opening locations plotted in Fig. 13 (where locations 1 and 2 had equal opening sizes, as did locations 3 and 4) were explored.

For the given range of S^*, higher C_L (lower k) values were observed under high turbulence approaching flows as shown in Fig. 14: this implied a higher damping ratio but a weaker resonant response for the increased turbulence. Since higher turbulence intensity was adopted during this wind tunnel test, it may also lead to larger loss coefficients in this paper relative to the established results in the previous study (Ginger and Holmes 2010, Holmes and Ginger 2012).

Under excitations of different external wind velocities, C_L values for opening A2 were identified and listed in Table 2 which indicated that the loss coefficient had strong correlation to the wind velocity and decreased significantly for increasing wind velocity. Therefore, more researches are needed to look further into the relationship between C_L and approaching wind velocity. Comparison of opening locations 1 to 4 in Table 3 demonstrated that corner opening 2 (near the side wall) produced the largest loss coefficient C_L or conversely the smallest k. As a matter of fact, changes of opening location were usually accompanied by variations of inflow turbulence which could be amplified at the airflow separation region just like in the case of opening location 2.

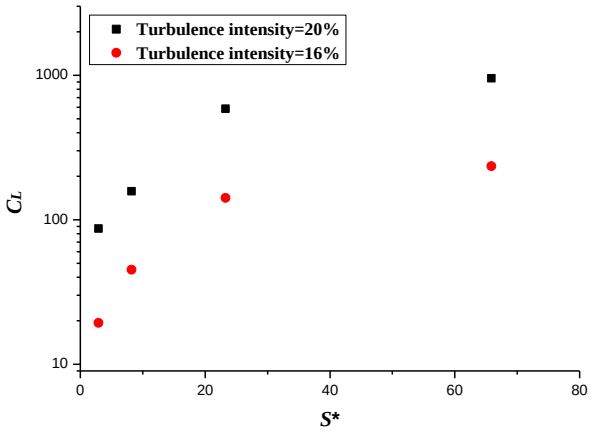

Fig. 14 C_L for different turbulence intensities

Table 2 Values of C_L for different wind velocities

A_0 (m^2)	Volume	I (%)	U (m/s)	C_L
0.01	V_0	20	12.8	500
0.01	V_0	20	7.5	1500

Table 3 Values of C_L for different opening locations

Opening location	1	2	3	4
S^*	4.3	4.3	1.5	1.5
C_L	17	31	13	15

5. Simplified loss coefficient formula

To describe the variation of loss coefficient with S^*, a simplified empirical formula was presented to give an approximation of C_L

$$C_L = \frac{1}{\left(a\log(b/S^*)+c\right)^2} \quad (S^* \le b) \tag{4a}$$

$$C_L = 1/(c)^2 \quad (S^* > b) \tag{4b}$$

where a, b, and c in Eq. (4) are adjustable constants. Parameter c determines the maximum (or minimum) level of C_L (or k) and is closely related to external wind characteristics and opening locations as discussed in the above study.

Appling the relationship $k = \sqrt{1/C_L}$ to derive the empirical expressions for the discharge coefficient k

$$k = a\log(b/S^*)+c \quad (S^* \le b) \tag{5a}$$

$$k = c \quad (S^* > b) \tag{5b}$$

C_L identified from this experiment dataset can be well fitted by

$$C_L = \frac{1}{\left(0.15\log(30/S^*)+0.07\right)^2} \quad (S^* \le 30) \tag{6a}$$

$$C_L = 1/(0.07)^2 \quad (S^* > 30) \tag{6b}$$

Comparing theoretically estimated and experimentally identified loss coefficients in Fig. 15 showed that two data sets agreed well with each other.

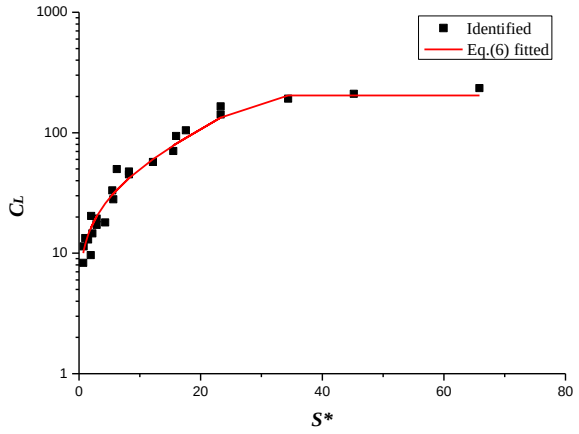

Fig. 15 Comparison of experimentally identified and theoretically estimated C_L

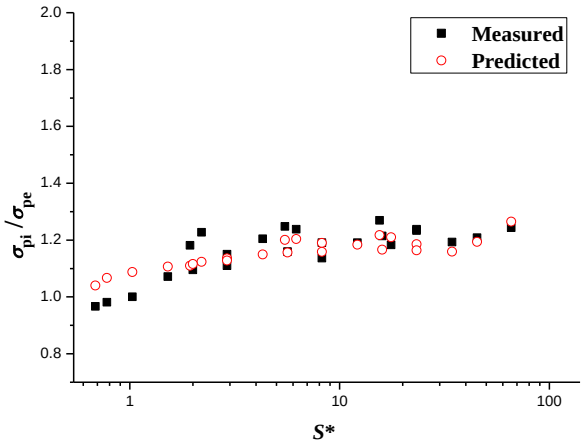

Fig. 16 Ratios of standard derivation of internal to external pressure

6. Prediction of the deviation ratio: internal to external pressure

Although the non-linear governing equation has high precision, it suffers a certain inconvenience in application for design purposes. Researchers including: Holmes and Ginger (2009, 2012), Vickery and Bloxham (1992), Irwin and Dunn (1994), Guha, Sharma *et al*. (2011), *inter alia* are among the first seeking simplified methods of estimating internal pressure responses.

Assuming that contribution of the Helmholtz resonance to internal pressure response was significant, Vickery and Bloxham (1992) used the linearised form of the governing equation to derive a relationship between $\sigma_{p\mathrm{i}}$ and $\sigma_{p\mathrm{e}}$

$$\frac{\sigma_{p\mathrm{i}}}{\sigma_{p\mathrm{e}}}=\left[(1-\alpha_c S_0)+(\frac{\pi^3 S_0^2}{32\beta^4\sigma_{C_{p\mathrm{e}}}^2})^{1/3}\right]^{1/2} \tag{7}$$

Here, α_c is an empirical parameter equal to 1.5 for Helmholtz frequencies located in the "five-thirds" range of the external pressure spectrum. $S_0 = f_{\mathrm{H}}S_{p\mathrm{e}}(f_{\mathrm{H}})/\sigma_{p\mathrm{e}}^2$ corresponds to the non-dimensional spectral density of the external pressure at its Helmholtz frequency, while parameter β is defined as $\frac{1}{2}\sqrt{\frac{C_L}{C_I}}\sqrt{\frac{1}{S^*}}$.

The accuracy of Eq. (7) largely depends upon the values of parameters C_I and C_L. Since the loss coefficient C_L varies with S^*, setting it to a constant value when applying Eq. (7) will be inappropriate. To verify validity of Eq. (7), the aforementioned wind tunnel test data were used. The inertial coefficients were determined from Helmholtz frequency, while the loss coefficients were approximated by Eq. (6). Using the non-dimensional Kaimal spectrum $S_0=\frac{200}{6}\frac{zf_H}{\overline{U}_z}/(1+50\frac{zf_H}{\overline{U}_z})^{5/3}$ combined with derived C_I and C_L, the ratios of standard deviation of internal to external pressure could be evaluated from Eq. (7). Fig. 16 compares calculated results with the experimental data. The predictions are satisfactory, albeit somewhat conservative for low values of S^*, suggesting the accuracy of Eq. (7) as acceptable.

7. Conclusions

The uncertain loss coefficient for fluctuating internal pressure inside a building with various dominant opening sizes and internal volumes were studied using wind tunnel tests. The importance of the parameter C_L in estimating internal pressure response was highlighted and the effects of building configurations (including: opening sizes, internal volumes, and opening locations) and approaching flow characteristics (wind velocity and turbulence intensity) on C_L were also explained. Based on experimental data-fitting, non-dimensional empirical formulae were developed to estimate loss coefficient of internal pressure resulting from a windward wall opening under normal onset flow conditions. Availability of the simplified prediction method for the ratios of standard deviation of internal to external pressure were evinced by measured data. The key conclusions were:

- Numerical study indicated that the internal pressure response in a building with a large opening but a small volume was more sensitive to variations of C_L values. The resonance effect of internal pressure decreased for increasing loss coefficient and became less sensitive to larger C_L value.
- C_L values were identified in terms of non-dimensional parameter S^* for a fixed range of Φ_5 values: it varied between 8 and 234.

- Changing the external wind field characteristics and opening locations significantly influenced the value of C_L. High turbulence flow, and an opening close to a sidewall may both result in large C_L values while increasing wind velocity causes C_L to reduce.
- An empirical function enabling the current experimentally identified C_L values to be fitted was presented. Further researches are needed to look into the three undetermined parameters (*a*, *b*, *c*) before this function can be used for design purpose.
- With accurate loss coefficients, simplified equation provided by Vickery and Bloxham for evaluating relationships of standard deviation between internal and the corresponding external pressure was proved to be applicable.

Acknowledgments

The work described in this paper was partially supported by China Postdoctoral Science Foundation (Project No. 2015M581938) and the National Natural Science Foundation of China (Project No. 51508502, 50908208). These supports are appreciated.

References

Architectural Institute of Japan (2004), *AIJ recommendations for loads on buildings*, Tokyo.

China Academy of Building Research (2002), *Load code for the design of building structures*, China.

Ginger, J.D., Holmes, J.D. and Kim, P.Y. (2010), "Variation of internal pressure with varying sizes of dominant openings and volumes", *J. Struct. Eng. - ASCE*, **136**(10), 1319-1326.

Ginger, J.D., Holmes, J.D. and Kopp, G.A. (2008), "Effect of building volume and opening size on fluctuating internal pressures", *Wind Struct*., **11**(5), 361-376.

Ginger, J.D., Mehta, K.C. and Yeatts, B.B. (1997), "Internal pressures in a low-rise full-scale building". *J. Wind. Eng. Ind. Aerod*., **72**, 163-174.

Guha, T.K., Sharma, R.N. and Richards, P.J. (2011), "Influence factors for wind induced internal pressure in a low rise building with a dominant opening", *Wind Eng*., **8**(2),1-17.

Holmes, J.D. (1979), "Mean and fluctuating pressures induced by wind", *Proceedings of the 5th International Conference on Wind Engineering*, Fort Collins, Colorado, USA, July.

Holmes, J.D. and Ginger, J.D. (2009), "Codification of internal pressure for building design", *Proceedings of the Seventh Asia-Pacific Conference on Wind Engineering*. Taipei, Taiwan, November.

Holmes, J.D. and Ginger, J.D. (2012), "Internal pressures-The dominant windward opening case - A review", *J. Wind. Eng. Ind. Aerod*., **100**(1), 70-76.

Irwin, P.A. and Dunn, G.E. (1994), "Review of internal pressures on low rise buildings", RWDI Report. 93-270, Canadian Sheet Steel Building Institute, Guelph, Ontario, Canada.

Liu, H. and Saathoff, P.J. (1981), "Building internal pressure: sudden change", *J. Eng. Mech. Div*., **107**, 109-321.

Oh, H.J., Kopp, G.A. and Inculet, D.R. (2007), "The UWO contribution to the NIST aerodynamic database for wind load on low buildings: Part 3.Internal pressure", *J. Wind. Eng. Ind. Aerod*., **95**(8), 755-779.

Sharma, R.N. and Richards, P.J. (1997a), "Computational modeling of the transient response of building internal pressure to a sudden opening" , *J. Wind. Eng. Ind. Aerod*., **72**, 149-161.

Sharma, R.N. and Richards, P.J. (1997b), "Computational modeling in the prediction of building internal pressure gain function", *J. Wind. Eng. Ind. Aerod*., **67-68**, 815-825.

Vickery, B.J. and Bloxham, C. (1992), "Internal pressure dynamics with a dominant opening", *J. Wind. Eng. Ind. Aerod*., **41**(1-3), 193-204.

Vickery, B.J.(1986), "Gust factors for internal pressures in low-rise buildings", *J. Wind. Eng. Ind. Aerod*., **23**, 259-271.
Xu, H.W., Yu, S.C. and Lou, W.J. (2014), "The inertial coefficient for fluctuating flow through a dominant opening in a building", *Wind Struct*., **18**(1), 57-67.
Yu, S.C., Lou, W.J. and Sun, B.N. (2006), "Wind-induced internal pressure fluctuations of structure with single windward wall opening", *J. Zhejiang University Science A*., **7**(3), 415-423.

CC